

## Analysis of the current intensity in each rotor bar of a squirrel cage induction motor: Case of a broken bar

Alexandre N'GUESSAN, Serge Mouroufié ADOU, and Abé Simon YAPI

Science and technology department, Laboratory of Technology (Lab-Tech), Félix Houphouët-Boigny University, Abidjan, Côte d'Ivoire

Copyright © 2024 ISSR Journals. This is an open access article distributed under the *Creative Commons Attribution License*, which permits unrestricted use, distribution, and reproduction in any medium, provided the original work is properly cited.

**ABSTRACT:** In view of the importance of squirrel cage induction machines in industrial applications, effective methods are needed to detect faults that could disrupt their operation. Despite their robustness, squirrel cage induction motors are subject to some faults, such as the broken bar. Current is one of the most widely used parameters for diagnosing squirrel cage induction motors. In most cases, however, the Motor Current Signature Analysis (MCSA) method is used. However, in the specific case of a broken bar, analysis of the current intensity in each rotor bar enables precise detection of a broken bar. The present work analyzes the evolution of the current intensity in each rotor bars in the case of a healthy rotor and in the presence of a broken bar. The current intensity in the rotor bar is strongly impacted, with a greatly reduced current. This situation also leads to a distribution of current intensity in the neighboring bars. As a result, the intensity of the current flowing through these bars increases according to their proximity to the faulty bar.

**KEYWORDS:** induction machine, rotor faults, diagnostic, rotor current, electrical system.

### 1 INTRODUCTION

The reliability of electrical systems, particularly in industry, is a major issue for service continuity [1], [2]. The squirrel cage induction machine is the type most commonly used in such systems [3], [4], [5]. In this type of machine, the rotor windings are replaced by conductor bars short-circuited at each end by short-circuit rings. Despite their robustness, squirrel cage induction motors are subject to several types of faults, including rotor faults in the electrical circuits [6], [7], [8]. The most commonly encountered faults are: partial or total breaking a short-circuit ring, partial or total broken bar. These faults are due to an accumulation of defects caused by certain stresses, notably electrical, mechanical, thermal and environmental. Fig. 1 shows the two main rotor faults of a squirrel cage induction machine.

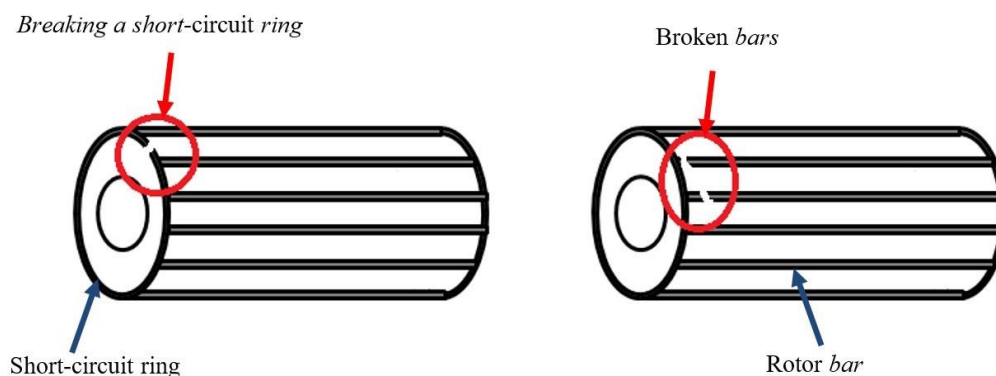


Fig. 1. Broken bars (circled in red) of the squirrel cage rotor

To anticipate the disastrous consequences of these faults, it is necessary to implement effective methods for early detection of this type of fault, which can disrupt the operation of these machines [9], [10]. The Motor Current Signature Analysis (MCSA) method is the most widely used method [11], [12], [13]. However, good results can also be obtained using other methods.

The aim of this article is to present the impact of a broken bar on rotor bar current. Results are presented for a squirrel cage induction motor operating with a healthy rotor, as well as for squirrel cage induction motor operating with a broken bar.

## 2 MATERIAL AND METHODS

### 2.1 ROTOR CAGE CIRCUIT

The rotor is made up of  $N_b$  rotor bars. The rotor can therefore be broken down into  $(N_b+1)$  independent electrical circuits. Each circuit is delimited by the two adjacent bars and the two short-circuit rings. One of the short-circuit rings creates an additional loop, bringing the number of electrical circuits to  $(N_b+1)$ . Each electrical circuit is studied independently of the others, with a current flowing through it. There are therefore  $(N_b+1)$  rotor currents. Bars and short-circuit rings are represented by a resistor in series with an inductor. The rotor of the squirrel cage induction motor can be represented as shown in Fig. 2 [5], [9], [19].

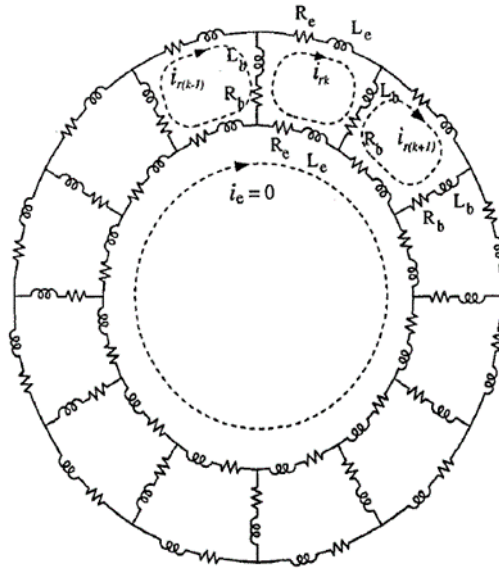


Fig. 2. Rotor of the squirrel cage induction motor

### 2.2 ROTOR MESH

The rotor of a squirrel cage induction motor can be represented by electrically interconnected and magnetically coupled meshes. A mesh is delimited by two bars and two short-circuit ring segments. Fig. 3 [5], [14], [15], [16], [17], [18], [19], shows a rotor mesh formed by two adjacent rotor bars ( $k$  and  $k-1$ ) and the short-circuit rings.

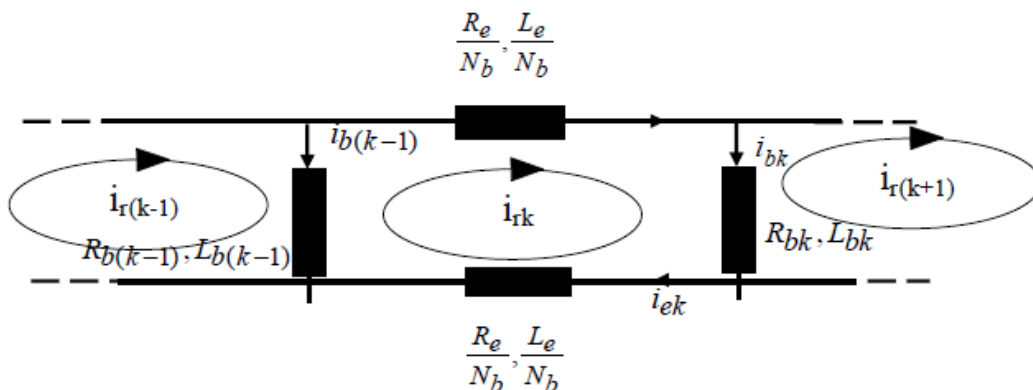


Fig. 3. Electric diagram equivalent of a rotor mesh

### 2.3 MODEL WITH BROKEN BAR

We can model the broken bar by cancelling the current flowing through it, even though several physical phenomena come into play during such a fault [14]. Fig. 4 [14] below shows a portion of the rotor cage with a broken bar.

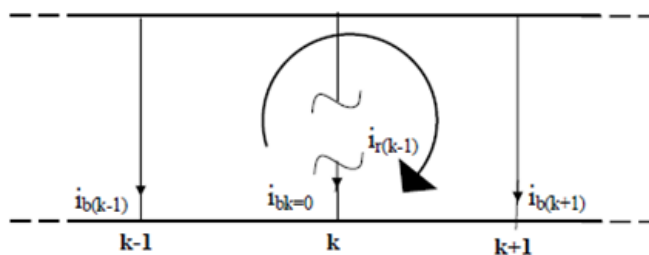


Fig. 4. Electric diagram of a rotor cage with a broken bar

Two approaches can be taken into account in this type of simulation. The first approach consists in reconstructing the rotor electrical circuit: the matrices are completely rebuilt. The order of the system is reduced and the current in the broken bar is entirely suppressed, while the current in the adjacent bars increases. This results in the addition of the two columns and rows related to the fault current.

The second approach is to increase the resistance value of the faulted bar sufficiently so that the current flowing through the bar in question is practically zero. In this second case, the self and mutual inductance matrices remain unchanged. This approach, which allows the simulation of partially broken bars, is more convenient and more realistic.

## 3 RESULTS AND DISCUSSION

### 3.1 HEALTHY ROTOR

At no load, the current in the rotor bars is practically zero. Under load, current intensity increases uniformly in all bars. Fig. 5 shows the maximum currents in the rotor bars for a healthy bar, from bar 1 to bar 26.

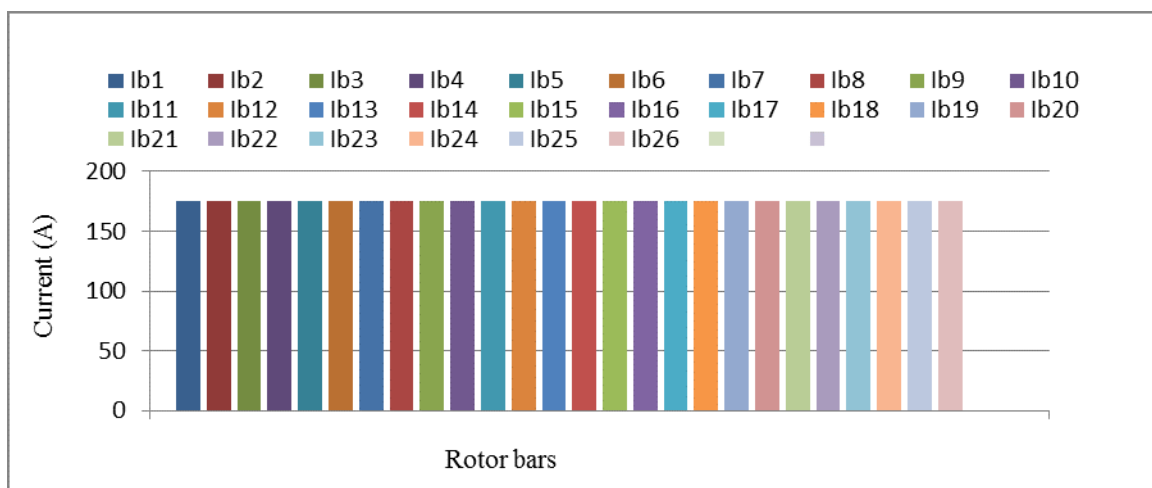


Fig. 5. Maximum currents in rotor bars (case of a healthy rotor)

### 3.2 ROTOR WITH A BROKEN BAR

In the presence of a broken bar, the currents in the various bars are no longer equal. They vary according to the position of the offending bar. The presence of a broken bar induces to overcurrent in the neighboring bars and a considerable reduction (close to zero) in the current intensity in the faulted bar (bar 12). Fig. 6 shows the maximum currents in the rotor bars in the event of a broken bar, from bar 1 to bar 26.

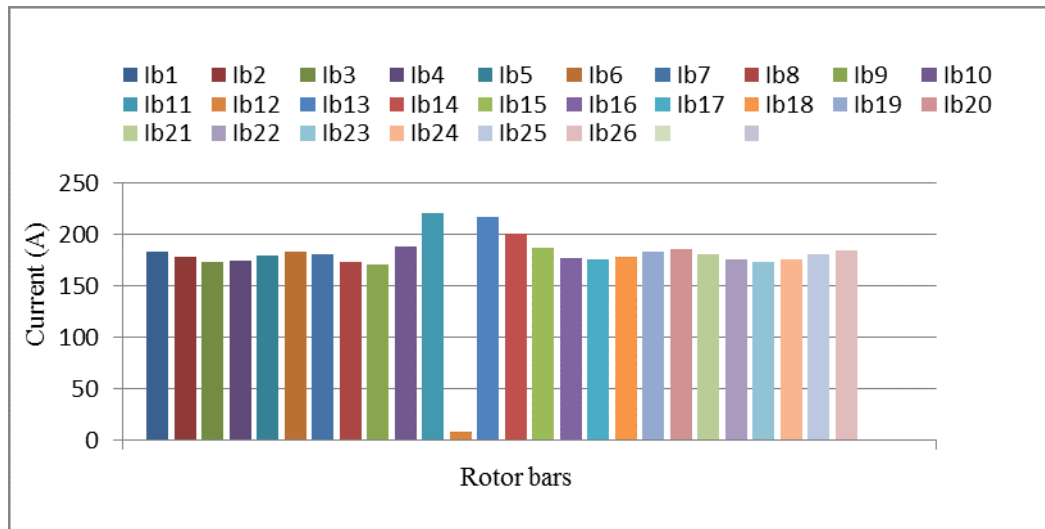


Fig. 6. Maximum currents in rotor bars following a broken bar (bar 12)

### 3.3 ROTOR WITH TWO NON-ADJACENT BROKEN BARS

In the case of two non-adjacent broken bars, the currents in the different bars are not equal. They vary according to the position of the offending bars. The presence of two broken bars leads to an overcurrent in the adjacent bars and a considerable reduction (close to zero) in the current in the faulted bars (bars 12 and 17). Fig. 7 shows the maximum currents in the rotor bars in the event of a broken bar, from bar 1 to bar 26.

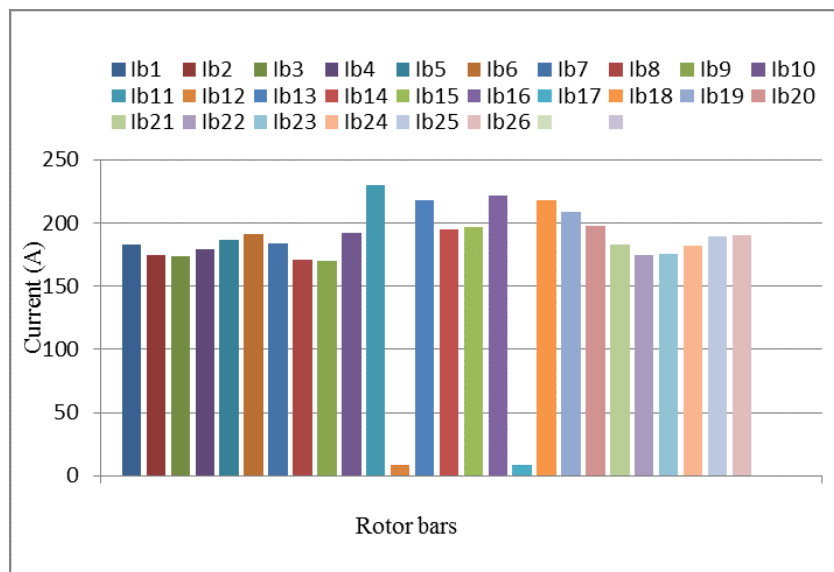


Fig. 7. Maximum currents in rotor bars following breakage of two non-adjacent rotor bars (bars 12 and 17)

### 3.4 ROTOR WITH TWO ADJACENT BROKEN BARS

In the case of two adjacent broken bars, the currents in the different bars also vary according to the position of the offending bars. The presence of two adjacent broken bars leads to an overcurrent in the adjacent bars and a considerable reduction (close to zero) of the current in the faulted bars (bars 12 and 13). Fig. 8 shows the maximum currents in the rotor bars in the event of a broken bar, from bar 1 to bar 26.

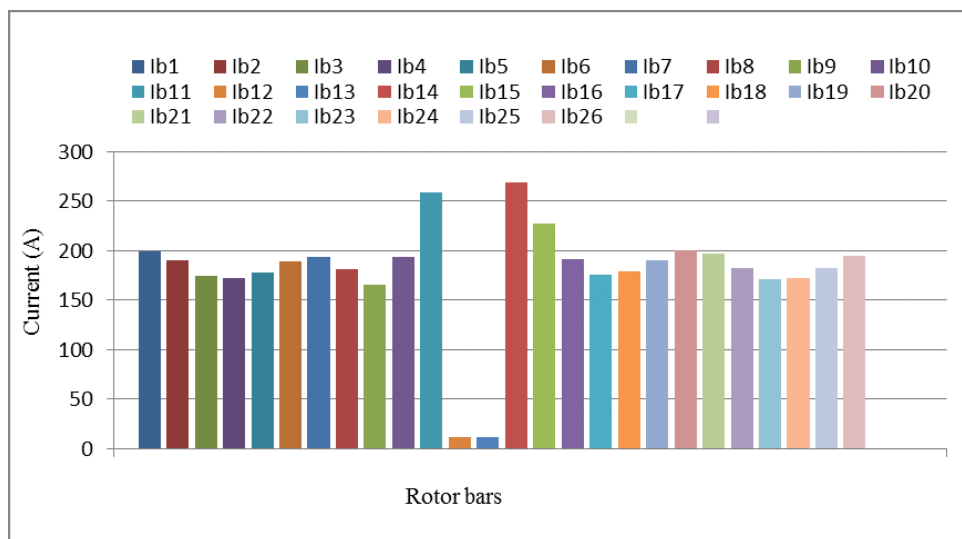


Fig. 8. Maximum currents in rotor bars following breakage of two adjacent rotor bars (bars 12 and 13)

### 3.5 EVOLUTION OF CURRENT INTENSITY

The current intensity in a rotor bar observes a transient regime before being cancelled out, as the motor runs at no load until 1s. Between 1s and 2s, a load with a torque of 10 N.m is applied to the motor. Oscillations due to the torque applied are observed at t=1s, leading to a maximum current of over 150 A, as shown in Figure 9. After the broken bar at t=2s, the current value drops sharply to around 11 A. A broken bar considerably reduces the current in the faulted bar. At t=3s, a second non-adjacent bar is broken, causing a very slight increase in bar current to 16 A. Fig. 9 shows the evolution of current intensity in a bar following a broken bar fault.

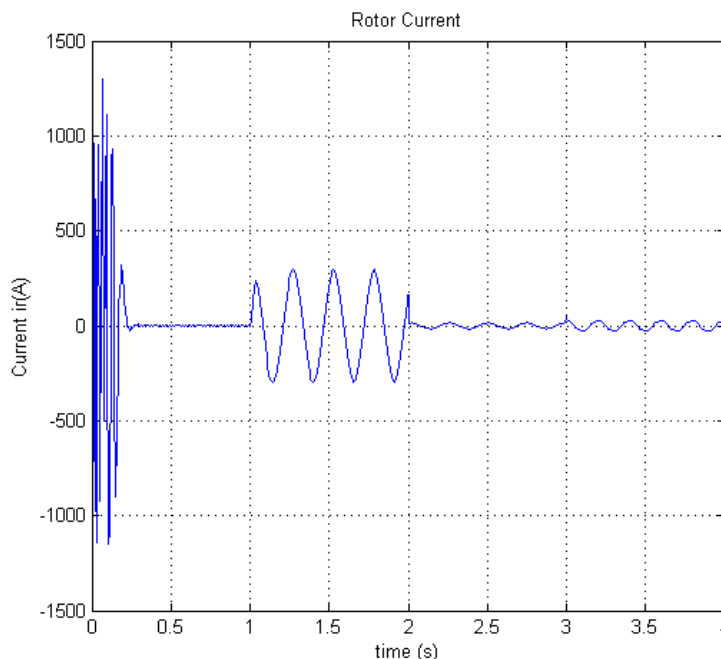


Fig. 9. Evolution of current intensity in a rotor bar

## 4 CONCLUSION

The aim of this article is to study the evolution of current intensity in each rotor bar for a healthy rotor and a rotor with a broken bar. First, the methodology used in this study was presented. Then, the various faults experienced by the squirrel cage induction motor at rotor level were studied. The broken bar is the one that has been particularly scrutinized since the study focuses on this fault. Finally, results showing the impact of a broken bar on the current intensity in each rotor bar were presented.

The results show that a broken bar drive to a considerable reduction in the current in the faulted bar, and a distribution of the current to the other bars, resulting in an increase in the current in the latter. This increase in current in the other bars is not uniform. Neighboring bars a greater increase than those further away. By analyzing the current in each rotor bar of a squirrel cage induction motor, a broken bar can be detected. The greatest difficulty lies in the difficult accessibility of the machine's rotor bars.

## NOMENCLATURE

$R_b$	Rotor bar resistance	$L_e/N_b$	Leakage inductance of short-circuit ring segment between two adjacent rotor bars
$L_b$	Leakage inductance of rotor bar	$i_{rk}$	Mesh current
$R_e$	Resistance of rotor short-circuit ring	$i_{bk}$	branch current
$R_e/N_b$	Resistance of short-circuit ring segment between two adjacent rotor bars	$i_{re}$	Short-circuit ring current
$L_e$	Leakage inductance of short-circuit ring rotor bar		

## APPENDIX

Parameters	Rated values	Unit (SI)
Output power	1500	W
Nominal voltage	230/400	V
Frequency	50	Hz
Inertia	$17.9 \times 10^{-3}$	Kg.m <sup>2</sup>
Number of rotor bars	26	
Number of turns per stator phase	367	
Number of pair of pole	2	
Leakage inductance of rotor short-circuit ring	$0.5033 \times 10^{-6}$	H
Rotor bar leakage inductance	$0.5033 \times 10^{-6}$	H
Rotor bar resistance	$80.67 \times 10^{-6}$	$\Omega$
Resistance of rotor short-circuit ring	$80.67 \times 10^{-6}$	$\Omega$
Resistance of the windings per stator phase	4.19	$\Omega$
Friction coefficient	$4.23 \times 10^{-3}$	N.m.s <sup>2</sup>
Cyclic inductance of the stator	$16.7 \times 10^{-3}$	H
Mutual stator-rotor inductance	$1.1226 \times 10^{-6}$	H

## REFERENCES

- [1] Romary, R., Thailly, D., Brudny, J.-F., and all, «Diagnostic de machines électriques par analyse du champ magnétique de dispersion», Revue de l'Électricité et de l'Électronique (REE), no. 11, pp. 49-62, 2006.
- [2] Movuela, M., R., «Apport de bruit de fond dans la détection des défauts dans le moteur asynchrone», International Journal of Innovation and Applied Studies, vol. 27, no. 1, pp. 190-201, 2006.
- [3] Bhowmik, P., S., «Fault diagnostic and monitoring methods of induction motor: A review», International Journal of Applied Control, Electrical and Electronics Engineering (IJACEEE), vol. 1, no. 1, pp. 1-18, 2013.
- [4] Blodt, M., Granjon, P., Raison, B., and Rostaing, G., «Models for Bearing Damage Detection in Induction Motors Using Stator Current Monitoring», IEEE Transaction on Industrial Electronics, vol. 55, no. 4, pp. 1813 – 1822, 2008.
- [5] Chouidira, I., Khodja, D., E., and Benguesnia, H., «Detection and diagnostic fault in machine asynchronous based on single processing», International Journal of Energetica (IJECA), vol. 4, no. 1, pp. 11-16, 2019.
- [6] Siddiqui, K., M., Sahay, K., and Giri, V., K., «Health Monitoring and Fault Diagnosis in Induction Motor- A Review», International Journal of Advanced Research in Electrical, Electronics and Instrumentation Engineering (IJAREEIE), vol. 3, no. 1, pp. 6549-6565, 2014.
- [7] Menacer, A., Champenois, G., Saïd, M., S., N., Benakeha, A., Moreau S., and Hassaine, S., «Rotor failures diagnosis of squirrel cage induction motors with different supplying sources», Journal of Electrical engineering & Technology, vol. 4, no. 2, pp. 219-228, 2009.
- [8] Pusca, R., Romary, R., Fireteanu, V., and Ceban, A., «Finite element analysis and experimental study of the near-magnetic field for detection of rotor faults in induction motors», Progress In Electromagnetics Research B., no. 50, pp. 37-59, 2013.

- [9] Lachitar, S., Ghozzal, A., Koussa, K., and all, «Broken rotor bar fault diagnostic for DTC fed induction motor using stator instantaneous complex apparent power envelope signature analysis», *International Journal of Power Electronics and Drive System (IJPEDS)*, vol. 10, no. 3, pp. 1187-1196, 2019.
- [10] Sanap, K., R., Paraskar, S., R., and Jadhao, S., S., «Broken rotor bar fault diagnosis of induction motor by signal processing techniques», *International journal of electrical engineering & technology (IJEET)*, vol. 8, no. 1, pp. 57-67, 2017.
- [11] Mellakhi, A., Benouzza, N., and Bendiabdellah, A., «Analyse spectrale du courant statorique pour détecter les cassures de barres dans les moteurs asynchrones triphasés à cage en tenant compte des harmoniques d'espace», *Nature et Technologie*, no. 2, pp. 35- 40, 2010.
- [12] Rigoni, M., Sadowski, N., Batistela, N., J., and Bastos, J., P., A., «Detection and analysis of rotor faults in induction motors by the measurement of the stray magnetic flux», *Journal of Microwaves, optoelectronics and electromagnetic applications*, vol. 11, no. 1, pp. 68-80, 2012.
- [13] Ceban, A., Pusca, R., and Romary, R., «Study of rotor faults in induction motors using external magnetic Field Analysis», *IEEE Transactions on industrial Electronics*, Vol. 59, No. 5, (2011), 2082-2093. <https://doi.org/10.1109/TIE.2011.2163285>.
- [14] Sahraoui, M., Zouzou, S., E., Menacer, A., Aboubou, A., et Derghal, A., «Diagnostic des défauts dans les moteurs asynchrones triphasés a cage, Partie II: Méthodes dédiées à la détection des cassures de barres dans les moteurs asynchrones triphasés a cage», *Courrier du Savoir*, No. 05, (2004), 57-61.
- [15] Aboubou, A., Shraoui, M., Zouzou, S., and all, «Comparaison de trois techniques dédiées au diagnostic des défauts rotoriques dans les moteurs asynchrones triphasés à cage», *Revue Internationale de Génie Électrique (RIGE)*, vol. 8, no. 3-4, pp. 557-576, 2005.
- [16] Kechida, R., Menacer, A., and Benakcha, A., «Fault Detection of Broken Rotor Bars Using Stator Current Spectrum for the Direct Torque Control Induction Motor», *World Academy of Science, Engineering and Technology*, vol. 4, no. 66, pp. 1244-1249, 2010.
- [17] Razik, H., «Le contenu spectral du courant absorbé par machine asynchrone en cas de défaillance, état de l'art» *La revue 3EI*, no. 29, pp. 48-52, 2002.
- [18] Shi, P., Chen, Z., and Yuriv Bagapov, «Modeling and analysis of induction machines under broken rotor-bar failures» *International Journal of Computer Applications*, vol. 69, no. 14, pp. 28-35, 2013.
- [19] Menacer, A., and Nait-Said, M., S., «Stator Current Analysis of incipient fault into Asynchronous motor rotor bars using Fourier fast transform, *Journal of Electrical Engineering*» vol. 55, no. 5-6, pp. 122-130, 2004.